J Biomol NMR (2014) 59:23–29
DOI 10.1007/s10858-014-9826-2

COMMUNICATION

Off-resonance rotating-frame relaxation dispersion experiment for ^{13}C in aromatic side chains using L-optimized TROSY-selection

Ulrich Weininger · Ulrika Brath · Kristofer Modig · Kaare Teilum · Mikael Akke

Received: 26 November 2013 / Accepted: 25 March 2014 / Published online: 5 April 2014

Abstract Protein dynamics on the microsecond–millisecond time scales often play a critical role in biological function. NMR relaxation dispersion experiments are powerful approaches for investigating biologically relevant dynamics with site-specific resolution, as shown by a growing number of publications on enzyme catalysis, protein folding, ligand binding, and allostery. To date, the majority of studies has probed the backbone amides or side-chain methyl groups, while experiments targeting other sites have been used more sparingly. Aromatic side chains are useful probes of protein dynamics, because they are over-represented in protein binding interfaces, have important catalytic roles in enzymes, and form a sizable part of the protein interior. Here we present an off-resonance $R_{1\rho}$ experiment for measuring microsecond to millisecond conformational exchange of aromatic side chains in selectively ^{13}C labeled proteins by means of longitudinal- and transverse-relaxation optimization. Using selective excitation and inversion of the narrow component of the ^{13}C doublet, the experiment achieves significant sensitivity enhancement in terms of both signal intensity and the fractional contribution from exchange to transverse relaxation; additional signal enhancement is achieved by optimizing the longitudinal relaxation recovery of the covalently attached ^{1}H spins. We validated the L-TROSY-selected $R_{1\rho}$ experiment by measuring exchange parameters for Y23 in bovine pancreatic trypsin inhibitor at a temperature of 328 K, where the ring flip is in the fast exchange regime with a mean waiting time between flips of 320 μs. The determined chemical shift difference matches perfectly with that measured from the NMR spectrum at lower temperatures, where separate peaks are observed for the two sites. We further show that potentially complicating effects of strong scalar coupling between protons (Weininger et al. in J Phys Chem B 117: 9241–9247, 2013b) can be accounted for using a simple expression, and provide recommendations for data acquisition when the studied system exhibits this behavior. The present method extends the repertoire of relaxation methods tailored for aromatic side chains by enabling studies of faster processes and improved control over artifacts due to strong coupling.

Keywords Conformational exchange · Strong coupling · Aromatic ring flip · Spin-lock

U. Weininger · U. Brath · K. Modig · M. Akke (✉)
Department of Biophysical Chemistry, Center for Molecular Protein Science, Lund University, P.O. Box 124, 22100 Lund, Sweden
e-mail: mikael.akke@bpc.lu.se

Present Address:
U. Brath
Department of Chemistry and Molecular Biology, University of Gothenburg, 41296 Göteborg, Sweden

K. Teilum
Department of Biology, University of Copenhagen, Ole Maaløes Vej 5, 2200 Copenhagen, Denmark

Conformational fluctuations in proteins on the microsecond to millisecond time scales are often linked to functional processes (Mittermaier and Kay 2006). Transitions between different conformations that lead to modulation of NMR parameters, such as the chemical shift (Gutowsky and Saika 1953) or residual dipolar couplings (Igumenova et al. 2007; Vallurupalli et al. 2007), result in exchange contributions to the transverse relaxation rate, which can be probed by NMR relaxation dispersion methods to yield unique information on the structures, thermodynamics and dynamics of the underlying process (Palmer et al. 2001;

Akke 2002). Experiments have been designed to probe conformational exchange at specific sites in proteins, including the backbone (Akke and Palmer 1996; Ishima et al. 1998, 2004; Loria et al. 1999a, b; Hill et al. 2000; Mulder and Akke 2003; Lundström and Akke 2005a, b; Igumenova and Palmer 2006; Lundström et al. 2009a) and side-chain aliphatic (Lundström et al. 2007b, 2009b; Hansen et al. 2012), methyl (Ishima et al. 1999; Mulder et al. 2002; Brath et al. 2006; Lundström et al. 2007b; Weininger et al. 2012b, 2013a), carbonyl/carboxyl (Paquin et al. 2008; Hansen and Kay 2011) and recently also aromatic groups (Teilum et al. 2006; Weininger et al. 2012c, 2013b).

Aromatic residues serve multiple functions in proteins. They commonly occur in protein binding interfaces, where they contribute a significant part of the binding free energy (Bogan and Thorn 1998; Lo Conte et al. 1999; Birtalan et al. 2010). Furthermore, His and Tyr play critical roles in enzyme catalytic mechanisms (Bartlett et al. 2002). Aromatic side chains contribute some 25 % of the protein interior volume, typically appearing in pairs or clusters where they form specific aromatic–aromatic interactions (Burley and Petsko 1985). Despite the generally tight packing of protein side chains, Phe and Tyr residues undergo frequent 180° rotations ('ring flips') of the χ^2 dihedral angle. For ring flips to occur, the available volume surrounding the ring must increase transiently (Wagner 1980; Karplus and McCammon 1981; Li et al. 1999). Therefore, aromatic residues are useful probes of the dynamics of the hydrophobic core. Indeed, studies of aromatic ring dynamics have a very long history in NMR, dating back to the 1970s when aromatic ring flips were first observed in proteins (Wüthrich and Wagner 1975; Campbell et al. 1975; Hull and Sykes 1975; Wagner et al. 1976) and has recently seen a renaissance (Skalicky et al. 2001; Sathyamoorthy et al. 2013; Weininger et al. 2013b; Kasinath et al. 2013).

Previous studies of ring-flip rates have largely been based on proton-detected lineshape analysis and various types of exchange spectroscopy (Li et al. 1999; Skalicky et al. 2001; Hattori et al. 2004; Rao and Bhuyan 2007). Recent developments have made it possible to study conformational dynamics of aromatic side-chains using heteronuclear relaxation rate measurements: site-specific ^{13}C labeling of proteins using 1-$^{13}C_1$-glucose or 2-$^{13}C_1$-glucose produces samples with isolated ^{13}C spins, thereby eliminating unwanted relaxation pathways and coherent magnetization transfer via one-bond couplings (Teilum et al. 2006; Lundström et al. 2007a) and enabling the first studies of conformational exchange of aromatic rings using $R_{1\rho}$ relaxation dispersion (Teilum et al. 2006). Alternative labeling strategies using 4-$^{13}C_1$-erythrose (Kasinath et al. 2013) or α-ketoacid precursors (Lichtenecker et al. 2013) in combination with deuteration lead to protein samples with higher isotope enrichment level and higher degree of isolation of the ^{1}H–^{13}C spin pairs in the aromatic rings of Phe and Tyr.

We recently introduced a suite of ^{13}C longitudinal and transverse relaxation-optimized (L-TROSY) based relaxation experiments, which offer improvements in signal-to-noise per unit time of at least 10–35 % (Weininger et al. 2012a). By measuring the relaxation of the narrow multiplet component, TROSY-type experiments significantly improve the relatively low sensitivity of aromatic ^{13}C spins towards exchange contributions to R_2 caused by their inherently fast transverse relaxation (approximately a factor of 4 greater than for a backbone ^{15}N spin) (Weininger et al. 2012c). We have shown that anomalous, 'upside-down' dispersion profiles recorded using the L-TROSY CPMG experiment are caused by strong ^{1}H-^{1}H couplings (Weininger et al. 2013b). In favorable cases, the anomalous dispersion profiles can be interpreted to determine slow ring-flip rates, even though the observed nuclei have near-degenerate chemical shifts in the two positions (Weininger et al. 2013b). These results clearly show that renewed interest in aromatic spin relaxation (Skalicky et al. 2001; Teilum et al. 2006; Boyer and Lee 2008; Weininger et al. 2012a, c; Kasinath et al. 2013) is rewarded by new insights into protein dynamics. To further expand the repertoire of spin relaxation experiments targeting aromatic rings, we introduce the ^{13}C L-TROSY-selected $R_{1\rho}$ experiment, which complements the corresponding CPMG-type experiment (Weininger et al. 2012c) by enabling studies of faster processes, as well as providing improved control over the effect of strong ^{1}H-^{1}H coupling on the acquired dispersion profiles.

We implemented L-TROSY in the context of the off-resonance $R_{1\rho}$ relaxation dispersion experiment (Akke and Palmer 1996; Zinn-Justin et al. 1997; Mulder et al. 1998; Evenäs et al. 2001), in order to study faster exchange processes involving aromatic rings. The pulse sequence (Fig. 1) uses the same general framework as the L-TROSY versions of the R_1, R_2, *NOE* (Weininger et al. 2012a) and CPMG dispersion experiments (Weininger et al. 2012c), where L-optimization is achieved by maintaining the water and aliphatic magnetizations along the $+z$-axis; see (Weininger et al. 2012a) for details. The present $R_{1\rho}$ relaxation experiment encompasses spin-state selection so as to spin-lock the narrow C_xH^α component of the ^{13}C doublet, as described previously for the analogous TROSY-selected $R_{1\rho}$ experiment developed for ^{15}N spins (Igumenova and Palmer 2006). The total relaxation period T is divided into two segments of equal length, interspersed by a ^{1}H decoupling element. In short, C_zH^α magnetization is initially generated at point A (Fig. 1) using a heteronuclear S^3E element (Meissner et al. 1997). The ^{13}C magnetization is then aligned along the effective field axis

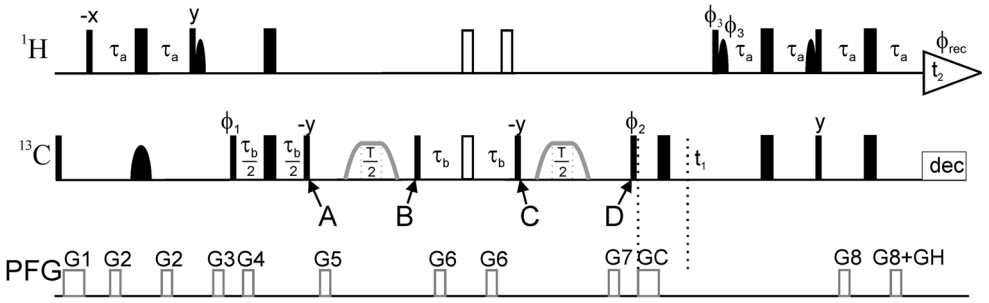

Fig. 1 Pulse sequence of the L-TROSY-$R_{1\rho}$ relaxation dispersion experiment for measuring conformational exchange of aromatic side chains in specifically ^{13}C labeled proteins. All pulses are applied along the *x axis* unless otherwise indicated. *Narrow* (*wide*) *solid bars* indicate rectangular high-power 90° (180°) pulses. *Open wide bars* indicate composite 180° pulses. The *continuous-wave* spin-lock relaxation periods T/2 and their flanking 4 ms tan/tanh adiabatic profiles are outlined in *gray* between points marked *A* and *B*, and *C* and D. The adiabatic sweep is initiated 25 kHz downfield or upfield of the spin-lock frequency. *Solid semi-ellipses* represent shaped pulses. *Narrow semi-ellipses* on ^{1}H are 90° EBURP2 (Geen and Freeman 1991) shapes centered at 1.9 ppm with a bandwidth of 6.6 ppm. The *wide semi-ellipse* on ^{13}C represents a 180° REBURP (Geen and Freeman 1991) pulse with a bandwidth of 40 ppm. ^{13}C is decoupled during acquisition using GARP (Shaka et al. 1985). The delays τ_a and τ_b are set to 1.5 and 1.4 ms, respectively. The magnetizations from water and aliphatic ^{1}H spins are aligned along the $+z$ axis whenever possible, including the spin-lock periods. The phase cycle is: $\phi_1 = 4(135°), 4(-45°)$, $\phi_2 = (y, x, -y, -x)$, $\phi_3 = (-y)$, $\phi_{rec} = (x, -y, -x, y, -x, y, x, -y)$. Pulsed field gradients G1–8 are employed to suppress unwanted coherences and artifacts, while GC and GH are encoding and decoding gradients, respectively, for echo/anti-echo coherence selection, obtained by inverting the signs of ϕ_3, GC and the even-numbered phases of the receiver. Gradient durations (in ms) and power levels (G/cm) are set to: G1 = (1.0, 10), G2 = (0.5, 8), G3 = (0.5, −20), G4 = (0.5, 6), G5 = (0.5, −10), G6 = (0.5, 12), G7 = (0.5, −40), G8 = (0.5, 18), GC = (1.0, 54), GH (0.5, 27.018). For every second t_1 increment, ϕ_2 and the receiver were incremented

using an adiabatic B_1 profile, spin-locked for a period $T/2$, and subsequently realigned along the z-axis at point B using a time-reversed adiabatic profile. ^{1}H inversion is achieved using an S^{3}CT element (Sorensen et al. 1997) between points B and C. Finally, the second half of the spin-lock period is executed identically to the first half, returning C_zH^α magnetization at point D. The present approach differs from that employed in the corresponding CPMG experiments (Loria et al. 1999b; Vallurupalli et al. 2007; Weininger et al. 2012c), which use an S^{3}CT element as the sole selection filter. The TROSY-selected off-resonance $R_{1\rho}$ experiment uses selective excitation, as well as selective inversion, of the slowly relaxing doublet component to minimize unwanted cross-relaxation effects (Igumenova and Palmer 2006), and also maintains a well-defined tilt-angle throughout the entire relaxation period, which further avoids artifacts (Korzhnev et al. 2002; Massi et al. 2004).

The TROSY effect for aromatic ^{13}C spins is expected to be near-optimal at a static magnetic field strength of $B_0 = 14.1$ T, as calculated based on the chemical shielding tensor for benzene (Veeman 1984) ($\sigma_{11} = 225$ ppm, $\sigma_{22} = 149$ ppm, $\sigma_{33} = 15$ ppm) and a C–H bond length of 1.08 Å. For reference, the estimated relaxation rate of the C_xH^α magnetization for an isotropically tumbling protein with an order parameter of $S^2 = 0.85$, varies between 8 and 30 s^{-1} for rotational correlation times in the range of 5–20 ns.

To validate the ^{13}C L-TROSY-selected $R_{1\rho}$ pulse sequence, we measured the ring-flip rate of Y23 in an 8 mM sample of natural abundance bovine pancreatic trypsin inhibitor (BPTI) (Wagner et al. 1976), dissolved in water pH 7.1, at a temperature of 55 °C and a static magnetic field strength of 11.7 T. Under these conditions, a single peak is observed for the δ spins, as well as the ε spins, and the ring flip is too fast to be determined accurately by CPMG relaxation dispersion (see Fig. 2). The advantage of benchmarking the performance of the $R_{1\rho}$ pulse sequence against aromatic ring flips in the fast exchange regime is that one can extract the chemical shift difference ($\Delta\delta$) from the product $\phi_{ex} = (\Delta\delta)^2 p_1 p_2$, since in this case the populations are known a priori ($p_1 = p_2 = 0.5$). Consequently, the value of $\Delta\delta$ determined from the $R_{1\rho}$ experiment can be directly compared to that determined from a spectrum recorded at lower temperature where the ring flip is in the slow exchange regime. Miloushev and Palmer have described a closed analytical formula for the specific case of symmetric two-state exchange in the fast exchange regime, expressing $R_{1\rho}$ as a function of the longitudinal relaxation rate (R_1), the exchange-free transverse relaxation rate ($R_{2,0}$), the exchange rate (k_{ex}), the chemical shift difference between the exchanging sites ($\Delta\delta$), and the effective field strengths of the two exchanging sites ($\omega_e = (\omega_1^2 + \Delta\Omega^2)^{1/2}$), which is the vector sum of the B_1 field strength (ω_1) and the off-resonance frequencies ($\Delta\Omega$), both of which are variables under experimental control (Miloushev and Palmer 2005).

Using the Miloushev-Palmer equation for the equal populations condition, we obtain a chemical shift difference for

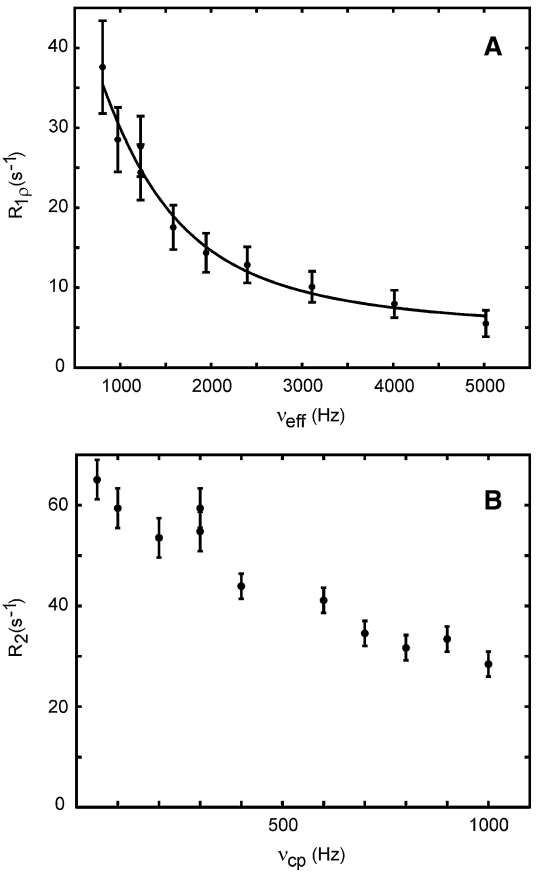

Fig. 2 ^{13}C aromatic L-TROSY-selected $R_{1\rho}$ (**a**) and CPMG (**b**) relaxation dispersion data for Y23 $^{13}C^{\varepsilon}$ acquired on an 8 mM sample of natural abundance BPTI in water pH 7.1 at 55 °C and a static magnetic field strength of 11.7 T. The $R_{1\rho}$ experiment was performed with the carrier placed on resonance with respect to the exchange-averaged ^{13}C signal. Data were fitted using the equation for symmetric exchange (Miloushev and Palmer 2005) and fixed populations, $p_1 = p_2 = 0.5$. The fitted parameters are $k_{ex} = (6.2 \pm 2.1) \times 10^3$ s^{-1} and $\Delta\delta = 1.43 \pm 0.09$ ppm

$^{13}C^{\varepsilon}$ of Y23 of $\Delta\delta = 1.43 \pm 0.09$ ppm and $k_{ex} = (6.2 \pm 2.1) \times 10^3$ s^{-1}. The chemical shift difference is in very good agreement with that measured ($\Delta\delta = 1.50$ ppm) at 5 and 15 °C, where Y23 is in slow exchange and separate signals from each side of the ring can be seen directly in the spectra; since the shift difference is virtually constant between 5 and 15 °C, we take this value to hold also at 55 °C. The stated errors correspond to one standard deviation, obtained by repeating the non-linear least square fit 1,000 times in a Monte-Carlo fashion (Press et al. 1986).

We have previously shown that aromatic ^{13}C L-TROSY CPMG relaxation dispersion experiments are affected by strong $^3J_{HH}$ couplings between the proton directly attached to the ^{13}C of interest and its vicinal ^{12}C-attached neighbor (Weininger et al. 2013b). Below, we outline the effect of strong $^3J_{HH}$ couplings in the context of the ^{13}C L-TROSY-selected $R_{1\rho}$ experiment, starting with a brief summary of the

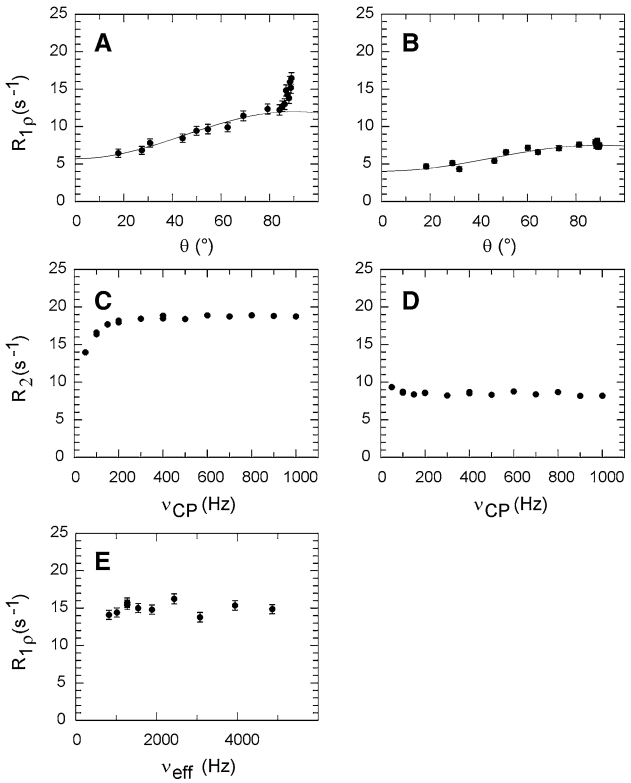

Fig. 3 Aromatic ^{13}C relaxation dispersion profiles of SlyD F79δ (**a**, **c**, **e**) and Y92δ (**b**, **d**). Neither of these residues are significantly influenced by exchange. H^{δ} and H^{ε} are strongly coupled in F79, but weakly coupled in Y92. **a**, **b** $R_{1\rho}$ relaxation dispersion shown as a function of the tilt angle θ. Data were fitted using the exchange-free expression $R_{1\rho} = R_1\cos^2(\theta) + R_2\sin^2(\theta)$ using $\theta < 80°$. **c**, **d** CPMG relaxation dispersion profiles. **e** On-resonance ($\theta = 90°$) $R_{1\rho}$ relaxation dispersion of F79δ. Data were acquired on a 1 mM sample of 1-$^{13}C_1$ glucose-labeled SlyD in 20 mM HEPES, pH 7.4 at 25 °C and a static magnetic field strength of 11.7 T

general conclusions presented previously. Strong $^3J_{HH}$ coupling leads to anomalous dispersion profiles, caused by modulation of the strong-coupling parameter ψ (defined by $\tan(2\psi) = {}^3J_{HH}/\Delta\nu$) as a function of the ^{13}C refocusing frequency (Weininger et al. 2013b), as exemplified in Fig. 3a, c. Phe, Tyr and the 6-ring moiety of Trp can be affected by strong couplings in principle, while His and the 5-ring moiety of Trp cannot, since the neighboring proton in each of the latter cases is attached to nitrogen and therefore resonates at a frequency far away from that of the ^{13}C-attached proton, i.e. $\Delta\nu_{HH} \gg {}^3J_{HH}$. The frequency difference between the two protons is given by $\Delta\nu = \Delta\nu_{HH} + {}^1J_{CH,eff}$, where $\Delta\nu_{HH}$ is the difference in resonance frequency between the ^{12}C-coupled proton and the central (decoupled) line of the ^{13}C-coupled proton (e.g. the δ and ε protons on each side of the ring in Phe and Tyr), and $^1J_{CH,eff}$ is the effective scalar coupling constant of the ^{1}H–^{13}C pair under the given ^{13}C decoupling conditions of the CPMG or spin-lock sequence. The ^{1}H-^{1}H scalar coupling constant is

essentially invariable in Phe and Tyr aromatic rings, $^3J_{HH} \approx 7$–8 Hz (Laatikainen et al. 1995), so that strong scalar coupling applies if $\Delta\nu < 2.5 \cdot {}^3J_{HH}$. To determine whether the strong-coupling condition applies on either side of the ring, one thus needs information on $\Delta\nu_{HH}$, which can be measured directly from the spectrum only if the ring-flip rate is slow enough that separate cross-peaks are observed for the two symmetric sites. In the case that only a single resonance is observed for each of the δ and ε protons (with ^{13}C decoupling), it is still possible to determine whether strong coupling applies to one or both sides of the ring, based on the observed chemical shift difference between the two protons, $\Delta\nu_{HH,obs} = (\Delta\nu_{HH,1} + \Delta\nu_{HH,2})/2 = (\nu_{\delta 1} - \nu_{\varepsilon 1} + \nu_{\delta 2} - \nu_{\varepsilon 2})/2$, and the criterion $\Delta\nu_{HH} < 2.5 \cdot {}^3J_{HH}$ (Weininger et al. 2013b); subscripts 1 and 2 denote the two sides of the ring. In the case of strong coupling on only one side of the ring, an anomalous dispersion profile implies that the ring-flip rate is quite slow (<200 s^{-1}), despite the appearance of a single cross-peak, since faster ring-flip rates effectively quench the strong coupling by exchange averaging (Weininger et al. 2013b).

To investigate the effect of strong couplings on $R_{1\rho}$ relaxation dispersions, we acquired off-resonance $R_{1\rho}$ data at different tilt angles (corresponding to different ^{13}C refocusing frequencies) on a 1 mM sample of 1-$^{13}C_1$ glucose-labeled SlyD from *Thermus thermophilus* (Löw et al. 2010), dissolved in 20 mM HEPES pH 7.4, at a temperature of 25 °C and a static magnetic field strength of 11.7 T. In SlyD, residue F79 exhibits strong $^3J_{HH}$ coupling on both sides of the ring (i.e., $\Delta\nu_{HH,1}$, $\Delta\nu_{HH,2} < 2.5 \cdot {}^3J_{HH}$), while all other aromatic residues are weakly coupled. (The δ and ε protons of Y23 in BPTI are weakly coupled on both sides of the ring; data not shown). As seen from Fig. 3a, strong coupling causes an anomalous increase in $R_{1\rho}$ relaxation rates of F79 for tilt angles $\theta > 80°$. This is a general result that is fully explained by the decoupling efficiency of the continuous-wave (cw) spin-lock field. The ^{13}C cw spin-lock field employed in the $R_{1\rho}$ experiment scales the splitting of the ^{13}C-coupled proton in a predictable manner according to $^1J_{CH,eff} = {}^1J_{CH}\, \Delta\Omega/(\omega_1^2 + \Delta\Omega^2)^{1/2} = {}^1J_{CH} \cos\theta$ (Shaka and Keeler 1987). We verified the expected dependence by measuring the residual splitting in the ^{1}H dimension of a ^{1}H–^{13}C HSQC acquired with off-resonance cw ^{13}C decoupling during acquisition (Fig. 4). In the case $\Delta\nu_{HH} \approx 0$, strong coupling thus arises for $^1J_{CH,eff} < 2.5 \cdot {}^3J_{HH}$, which translates to tilt angles $\theta > 80°$ (Fig. 4). As evident from Fig. 3a, it is quite straightforward in this case to identify the effect of strong coupling in the $R_{1\rho}$ experiment and subsequently exclude data points at $\theta > 80°$ from further analysis. In cases where $\Delta\nu_{HH} \neq 0$, the strong coupling scenario might be reached at intermediate values of θ, but typically affects only a single point on the relaxation dispersion curve (data not shown), which can be omitted provided that it can

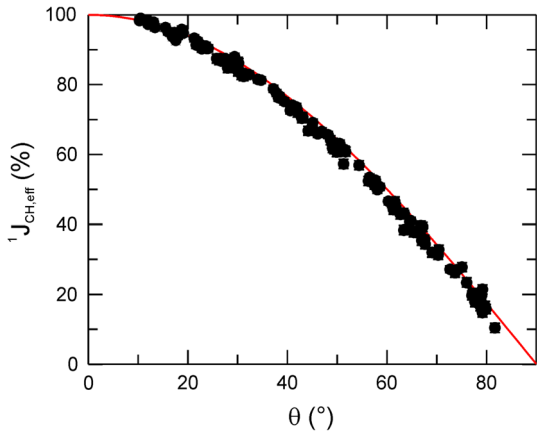

Fig. 4 The relative effective ^{1}H-^{13}C scalar coupling constant, $^1J_{CH,eff}$ (%), plotted as a function of the tilt angle θ. The expected dependence $^1J_{CH,eff} = {}^1J_{CH} \cos\theta$ is indicated as a *solid*, *red line*. Data were acquired using cw ^{13}C decoupling during the acquisition of aromatic ^{1}H–^{13}C-HSQC spectra on a 1 mM sample of 1-$^{13}C_1$ glucose-labeled SlyD in 20 mM HEPES, pH 7.4 at 25 °C, and a static magnetic field strength of 11.7 T

be reliably identified. Alternatively, the effects of strong-coupling artifacts on individual data points can be mitigated by acquiring $R_{1\rho}$ dispersion data using a fixed tilt angle but variable effective field strength. In this case strong coupling increases the measured $R_{1\rho}$ rates by a constant value that does not influence the final dispersion profile, as exemplified by Fig. 3e. This approach is advantageously performed on-resonance for cases where $\Delta\nu_{HH} \neq 0$, which yields the greatest exchange contributions to the measured $R_{1\rho}$ rates, while a value of $\theta \approx 80°$ should be near-optimal for $\Delta\nu_{HH} \approx 0$. Thus, the $R_{1\rho}$ experiment offers a higher level of control over the effects of strong $^3J_{HH}$ coupling on the dispersion profile than what is possible in CPMG experiments, where decoupling generates sidebands that modulate the splitting of the ^{1}H resonances in a manner that cannot be predicted quantitatively without numerical simulations (Weininger et al. 2013b; Eden et al. 1996).

In conclusion, the ^{13}C L-TROSY-selected $R_{1\rho}$ pulse sequence enables accurate measurements of conformational exchange affecting aromatic rings. The effect of strong ^{1}H-^{1}H scalar couplings on the dispersion profile can be predicted reliably using a closed analytical expression describing the ^{13}C decoupling efficiency during the spin-lock and prior knowledge of the ^{1}H spectrum. The new pulse sequence complements previous experiments, such as the L-TROSY CPMG dispersion experiment, by extending the accessible range of exchange processes towards faster rates and by offering additional advantages intrinsic to rotating-frame experiments (Palmer and Massi 2006).

Acknowledgments We thank Bertil Halle for the BPTI sample. This research was supported by the Swedish Research Council (621-2010-4912; 822-2005-2915), the Göran Gustafsson Foundation for

Research in Natural Sciences and Medicine, and the Knut and Alice Wallenberg Foundation. U.W. was supported by an EMBO long-term fellowship.

References

Akke M (2002) NMR methods for characterizing microsecond–millisecond dynamics in recognition and catalysis. Curr Opin Struct Biol 12:642–647

Akke M, Palmer AG (1996) Monitoring macromolecular motions on microsecond–millisecond time scales by $R_{1\rho} - R_1$ constant-relaxation-time NMR spectroscopy. J Am Chem Soc 118:911–912

Bartlett GJ, Porter CT, Borkakoti N, Thornton JM (2002) Analysis of catalytic residues in enzyme active sites. J Mol Biol 324(1):105–121

Birtalan S, Fisher RD, Sidhu SS (2010) The functional capacity of the natural amino acids for molecular recognition. Mol BioSyst 6(7): 1186–1194

Bogan AA, Thorn KS (1998) Anatomy of hot spots in protein interfaces. J Mol Biol 280(1):1–9

Boyer JA, Lee AL (2008) Monitoring aromatic picosecond to nanosecond dynamics in proteins via 13C relaxation: expanding perturbation mapping of the rigidifying core mutation V54A in Eglin C. Biochemistry 47:4876–4886

Brath U, Akke M, Yang D, Kay LE, Mulder FAA (2006) Functional dynamics of human FKBP12 revealed by methyl 13C rotating frame relaxation dispersion NMR spectroscopy. J Am Chem Soc 128:5718–5727

Burley SK, Petsko GA (1985) Aromatic-aromatic interaction—a mechanism of protein-structure stabilization. Science 229(4708):23–28

Campbell ID, Dobson CM, Williams RJP (1975) Proton magnetic resonance studies of the tyrosine residues of hen lysozyme—assignment and detection of conformational mobility. Proc R Soc Lond B 189:503–509

Eden M, Lee YK, Levitt MH (1996) Efficient simulation of periodic problems in NMR. Application to decoupling and rotational resonance. J Magn Reson, Ser A 120(1):56–71

Evenäs J, Malmendal A, Akke M (2001) Dynamics of the transition between open and closed conformations in a calmodulin C-terminal domain mutant. Structure 9:185–195

Geen H, Freeman R (1991) Band-selective radiofrequency pulses. J Magn Reson 93:93–141

Gutowsky HS, Saika A (1953) Dissociation, chemical exchange, and the proton magnetic resonance in some aqueous electrolytes. J Chem Phys 21(10):1688–1694

Hansen AL, Kay LE (2011) Quantifying millisecond time-scale exchange in proteins by CPMG relaxation dispersion NMR spectroscopy of side-chain carbonyl groups. J Biomol NMR 50(4):347–355

Hansen AL, Lundström P, Velyvis A, Kay LE (2012) Quantifying millisecond exchange dynamics in proteins by CPMG relaxation dispersion NMR using side-chain H-1 probes. J Am Chem Soc 134(6):3178–3189

Hattori M, Li H, Yamada H, Akasaka K, Hengstenberg W, Gronwald W, Kalbitzer HR (2004) Infrequent cavity-forming fluctuations in HPr from staphylococcus carnosus revealed by pressure- and temperature-dependent tyrosine ring flips. Prot Sci 13(12):3104–3114

Hill RB, Bracken C, DeGrado WF, Palmer AG (2000) Molecular motions and protein folding: characterization of the backbone dynamics and folding equilibrium of alpha D-2 using C-13 NMR spin relaxation. J Am Chem Soc 122(47):11610–11619

Hull WE, Sykes BD (1975) Fluorotyrosine alkaline phosphatase. Internal mobility of individual tyrosines and the role of chemical shift anisotropy as a fluorine-19 nuclear spin relaxation mechanism in proteins. J Mol Biol 98:121–153

Igumenova TI, Palmer AG (2006) Off-resonance TROSY-selected R1r experiment with improved sensitivity for medium- and high-molecular-weight proteins. J Am Chem Soc 128:8110–8111

Igumenova TI, Brath U, Akke M, Palmer AG (2007) Characterization of chemical exchange using residual dipolar coupling. J Am Chem Soc 129:13396–13397

Ishima R, Wingfield PT, Stahl SJ, Kaufman JD, Torchia DA (1998) Using amide 1H and 15 N transverse relaxation to detect millisecond time-scale motions in perdeuterated proteins: application to HIV-1 protease. J Am Chem Soc 120:10534–10542

Ishima R, Louis JM, Torchia DA (1999) Transverse ^{13}C relaxation of CHD_2 methyl isotopomers to detect slow conformational changes of protein side chains. J Am Chem Soc 121:11589–11590

Ishima R, Baber J, Louis JM, Torchia DA (2004) Carbonyl carbon transverse relaxation dispersion measurements and ms–ms timescale motion in a protein hydrogen bond network. J Biomol NMR 29:187–198

Karplus M, McCammon JA (1981) Pressure-dependence of aromatic ring rotations in proteins—a collisional interpretation. FEBS Lett 131(1):34–36

Kasinath V, Valentine KG, Wand AJ (2013) A 13C labeling strategy reveals a range of aromatic side chain motion in calmodulin. J Am Chem Soc 135:9560–9563

Korzhnev DM, Skrynnikov NR, Millet O, Torchia DA, Kay LE (2002) An NMR experiment for the accurate measurement of heteronuclear spin-lock relaxation rates. J Am Chem Soc 124(36):10743–10753

Laatikainen R, Ratilainen J, Sebastian R, Santa H (1995) NMR-study of aromatic–aromatic interactions for benzene and some other fundamental aromatic systems using alignment of aromatics in strong magnetic-field. J Am Chem Soc 117(44):11006–11010

Li H, Yamada H, Akasaka K (1999) Effect of pressure on the tertiary structure and dynamics of folded basic pancreatic trypsin inhibitor. Biophys J 77(5):2801–2812

Lichtenecker RJ, Weinhäupl K, Schmid W, Konrat R (2013) a-Ketoacids as precursors for phenylalanine and tyrosine labelling in cell-based protein overexpression. J Biomol NMR 57:205–209

Lo Conte L, Chothia C, Janin J (1999) The atomic structure of protein–protein recognition sites. J Mol Biol 285(5):2177–2198

Loria JP, Rance M, Palmer AG (1999a) A relaxation-compensated Carr-Purcell-Meiboom-Gill sequence for characterizing chemical exchange by NMR spectroscopy. J Am Chem Soc 121:2331–2332

Loria JP, Rance M, Palmer AG (1999b) A TROSY CPMG sequence for characterizing chemical exchange in large proteins. J Biomol NMR 15:151–155

Löw C, Neumann P, Tidow H, Weininger U, Haupt C, Friedrich-Epler B, Scholz C, Stubbs MT, Balbach J (2010) Crystal structure determination and functional characterization of the metallochaperone SlyD from *Thermus thermophilus*. J Mol Biol 398(3):375–390

Lundström P, Akke M (2005a) Microsecond protein dynamics measured by rotating-frame $^{13}C^{a}$ spin relaxation. ChemBioChem 6:1685–1692

Lundström P, Akke M (2005b) Off-resonance rotating-frame amide proton spin relaxation experiments measuring microsecond chemical exchange in proteins. J Biomol NMR 32:163–173

Lundström P, Teilum K, Carstensen T, Bezsonova I, Wiesner S, Hansen F, Religa TL, Akke M, Kay LE (2007a) Fractional 13C

enrichment of isolated carbons using [1-13C]- or [2-13C]-glucose facilitates the accurate measurement of dynamics at backbone Ca and side-chain methyl positions in proteins. J Biomol NMR 38:199–212

Lundström P, Vallurupalli P, Religa TL, Dahlquist FW, Kay LE (2007b) A single-quantum methyl C-13-relaxation dispersion experiment with improved sensitivity. J Biomol NMR 38(1):79–88

Lundström P, Hansen DF, Vallurupalli P, Kay LE (2009a) Accurate measurement of alpha proton chemical shifts of excited protein states by relaxation dispersion NMR spectroscopy. J Am Chem Soc 131(5):1915–1926

Lundström P, Lin H, Kay LE (2009b) Measuring $^{13}C^{\beta}$ chemical shifts of invisible excited states in proteins by relaxation dispersion NMR spectroscopy. J Biomol NMR 44(3):139–155

Massi F, Johnson E, Wang C, Rance M, Palmer AG (2004) NMR R_{1r} rotating-frame relaxation with weak radio frequency fields. J Am Chem Soc 126:2247–2258

Meissner A, Duus JO, Sorensen OW (1997) Spin-state-selective excitation. Application for E.COSY-type measurement of J_{HH} coupling constants. J Magn Reson 128(1):92–97

Miloushev VZ, Palmer AG (2005) R(1p) relaxation for two-site chemical exchange: general approximations and some exact solutions. J Magn Reson 177(2):221–227

Mittermaier A, Kay LE (2006) New tools provide new insights in NMR studies of protein dynamics. Science 312:224–228

Mulder FAA, Akke M (2003) Carbonyl 13C transverse relaxation measurements to sample protein backbone dynamics. Magn Reson Chem 41:853–865

Mulder FAA, de Graaf RA, Kaptein R, Boelens R (1998) An off-resonance rotating frame relaxation experiment for the investigation of macromolecular dynamics using adiabatic rotations. J Magn Reson 131(2):351–357

Mulder FAA, Hon B, Mittermaier A, Dahlquist FW, Kay LE (2002) Slow internal dynamics in proteins: application of NMR relaxation dispersion spectroscopy to methyl groups in a cavity mutant of T4 lysozyme. J Am Chem Soc 124:1443–1451

Palmer AG, Massi F (2006) Characterization of the dynamics of biomacromolecules using rotating-frame spin relaxation NMR spectroscopy. Chem Rev 106:1700–1719

Palmer AG, Kroenke CD, Loria JP (2001) Nuclear magnetic resonance methods for quantifying microsecond-to-millisecond motions in biological macromolecules. Methods Enzymol 339:204–238

Paquin R, Ferrage F, Mulder FAA, Akke M, Bodenhausen G (2008) Multiple-timescale dynamics of side-chain carboxyl and carbonyl groups in proteins by C-13 nuclear spin relaxation. J Am Chem Soc 130(47):15805

Press WH, Flannery BP, Teukolsky SA, Vetterling WT (1986) Numerical recipes. The art of scientific computing. Cambridge University Press, Cambridge

Rao DK, Bhuyan AK (2007) Complexity of aromatic ring-flip motions in proteins: Y97 ring dynamics in cytochrome c observed by cross-relaxation suppressed exchange NMR spectroscopy. J Biomol NMR 39(3):187–196

Sathyamoorthy B, Singarapu KK, Garcia AE, Szyperski T (2013) Protein conformational space populated in solution probed with aromatic residual dipolar 13C-1H couplings. ChemBioChem 14:685–688

Shaka AJ, Keeler J (1987) Broadband spin decoupling in isotropic liquids. Prog NMR Spectrosc 19:47–129

Shaka AJ, Barker PB, Freeman R (1985) Computer-optimized decoupling scheme for wideband applications and low-level operation. J Magn Reson 64:547–552

Skalicky JJ, Mills JL, Sharma S, Szyperski T (2001) Aromatic ring-flipping in supercooled water: implications for NMR-based structural biology of proteins. J Am Chem Soc 123(3):388–397

Sorensen MD, Meissner A, Sorensen OW (1997) Spin-state-selective coherence transfer via intermediate states of two-spin coherence in IS spin systems: application to E.COSY-type measurement of J coupling constants. J Biomol NMR 10(2):181–186

Teilum K, Brath U, Lundström P, Akke M (2006) Biosynthetic 13C labeling of aromatic side-chains in proteins for NMR relaxation measurements. J Am Chem Soc 128:2506–2507

Vallurupalli P, Hansen DF, Stollar E, Meirovitch E, Kay LE (2007) Measurement of bond vector orientations in invisible excited states of proteins. Proc Natl Acad Sci USA 104:18473–18477

Veeman WS (1984) Carbon-13 chemical shift anisotropy. Prog NMR Spectrosc 16:193–235

Wagner G (1980) Activation volumes for the rotational motion of interior aromatic rings in globular-proteins determined by high-resolution H-1-NMR at variable pressure. FEBS Lett 112(2):280–284

Wagner G, Demarco A, Wüthrich K (1976) Dynamics of aromatic amino-acid residues in globular conformation of basic pancreatic trypsin-inhibitor (Bpti).1. H-1 NMR-studies. Biophys Struct Mech 2(2):139–158

Weininger U, Diehl C, Akke M (2012a) 13C relaxation experiments for aromatic side chains employing longitudinal- and transverse-relaxation optimized NMR spectroscopy. J Biomol NMR 53:181–190

Weininger U, Liu Z, McIntyre DD, Vogel HJ, Akke M (2012b) Specific $^{12}C^{\beta}D_2^{12}C^{\gamma}D_2S^{13}C^{\varepsilon}HD_2$ isotopomer labeling of methionine to characterize protein dynamics by 1H and 13C NMR relaxation dispersion. J Am Chem Soc 134:18562–18565

Weininger U, Respondek M, Akke M (2012c) Conformational exchange of aromatic side chains characterized by L-optimized TROSY-selected 13C CPMG relaxation dispersion. J Biomol NMR 54:9–14

Weininger U, Blissing AT, Hennig J, Ahlner A, Liu ZH, Vogel HJ, Akke M, Lundstrom P (2013a) Protein conformational exchange measured by $^{1}HR_{1\rho}$ relaxation dispersion of methyl groups. J Biomol NMR 57:47–55

Weininger U, Respondek M, Löw C, Akke M (2013b) Slow aromatic ring flips detected despite near-degenerate NMR frequencies of the exchanging nuclei. J Phys Chem B 117:9241–9247

Wüthrich K, Wagner G (1975) NMR investigations of the dynamics of the aromatic amino acid residues in the basic pancreatic trypsin inhibitor. FEBS Lett 50:265–268

Zinn-Justin S, Berthault P, Guenneugues M, Desvaux H (1997) Off-resonance rf fields in heteronuclear NMR: application to the study of slow motions. J Biomol NMR 10:363–372